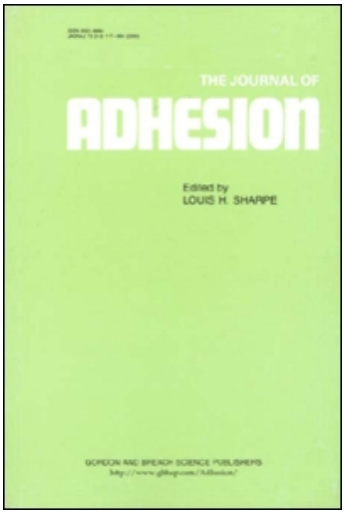

The Journal of Adhesion

Publication details, including instructions for authors and subscription information:
http://www.informaworld.com/smpp/title~content=t713453635

Microcrack Initiation in Adhesive Bonded Double-lap Joints with Scarfed Ends of Outer Adherends

Y. Gilibert[a]; M. L. L. Klein[a]
[a] Groupe Composites et Collage, Laboratoire de Mécanique et Energétique, Ecole Nationale Supérieure de Techniques, Avancées, Palaiseau, France

To cite this Article Gilibert, Y. and Klein, M. L. L.(1989) 'Microcrack Initiation in Adhesive Bonded Double-lap Joints with Scarfed Ends of Outer Adherends', The Journal of Adhesion, 28: 1, 51 — 69
To link to this Article: DOI: 10.1080/00218468908030169
URL: http://dx.doi.org/10.1080/00218468908030169

J. Adhesion, 1989, Vol. 28, pp. 51–69
Reprints available directly from the publisher
Photocopying permitted by license only

Printed in the United Kingdom

Microcrack Initiation in Adhesive Bonded Double-lap Joints with Scarfed Ends of Outer Adherends†

Y. GILIBERT‡ and M. L. L. KLEIN

Groupe Composites et Collage, Laboratoire de Mécanique et Energétique, Ecole Nationale Supérieure de Techniques Avancées 91120 Palaiseau, France

(Received June 14, 1988; in final form December 10, 1988)

Strain-gauge methods show how the scarfing of outer adherends influence the thresholds for microcrack initiation and flaw propagation in an adhesive-bonded, double-lap joint. There is an optimal value for the angle of the free ends that gives the sample, undergoing shear obtained by loading in direct traction, a very good mechanical strength.

A simplified solution can be calculated from the hypothesis of pure traction of the adherends, which is comparable with the microstrain profile. A numerical method is also obtained for quasi-linear evaluation of the shear modulus of the adhesive joint.

KEY WORDS Adhesive bonded joint; double-lap; scarfed joint; optimization; experiment; theory; damage mechanism; shearing; tearing.

1 INTRODUCTION

The double-lap joint, represented in Figures 1 and 2, has been used in the non-scarfed case ($l_2 = e_s$) to study the quality and strength of the joint. Experiments with the optimal model, that maximizes the ultimate load for a given core thickness, have shown that the classical theory, in which adherends are stressed in traction, is a good approximation in the linear range.

However, the extensometric method has brought to the fore the local perturbations caused by internal damage of the adhesive joint, studied by Gilibert.[1]

The researches that we have conducted on plane or axisymmetrical composite materials, have enabled us to refine our experimental method. It is based upon

† Presented at the International Conference, "Adhesion '87" of the Plastics and Rubber Institute held at York University, England, September 7–9, 1987.

‡ Corresponding author, whose address is: Université de REIMS, I.U.T. GENIE CIVIL 51100 REIMS, France.

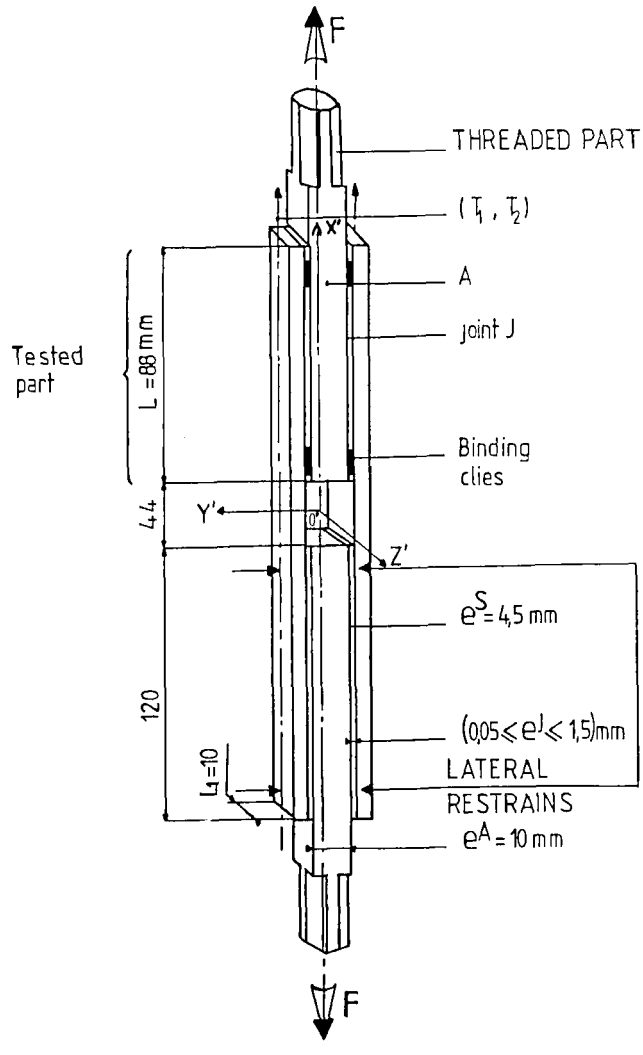

FIGURE 1 Traction test specimen.

measurements of the surface strains of the loaded test specimen, by the means of electric strain gauges. (See Chapter VIII of Reference 1).

We get reliable, precise and accurate results, which can be satisfactorily reproduced. Moreover, to treat any problems encountered, we have designed and developed new tools,[2,3,4] where existing techniques were inadequate. The experimental investigation is the best way to give prominence to the basic facts, in fields where the classical and theoretical approach of continuum mechanics is often not suitable.[5,6,7,8]

In Section 2 we describe how test specimens were constructed. Then, we

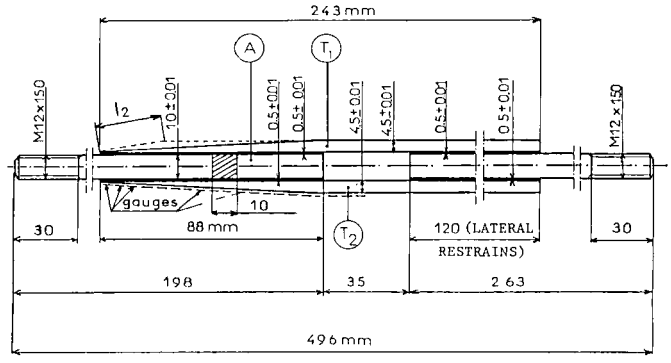

FIGURE 2 Double shear joint, with scarfed ends of outer adherends.

present the results of a theoretical and experimental analysis of the mechanical behaviour of the unbevelled double-lap. Sections 4 and 5 are devoted to the analysis of the influence of the bevel angle of the steel sheets on the mechanical behaviour of the specimen.

2 EXPERIMENTAL ASPECTS

2.1 Unbevelled double-lap (UBDL)

The type of samples used (Figure 1) is as follows:

a) For adherends we have used a low carbon steel (0.18% carbon; XC 18 French standard, equivalent to SAE-AISI 1017) of uniform quality, the characteristics of which have been measured by an extensometric method in a tensile test:

$E_T = E_A = 207700 \pm 10$ MPa, $\nu_T = \nu_A = 0.288 \pm 0.003$ (the strain gauges were installed on steel rods, 25 cm long and 1 cm square cross section. The pickup was of the type WA 06120 WT VISHAY MICRO-MEASUREMENTS). The loading rate was close to 100 daN mn^{-1} ($\dot{\varepsilon} = 10^{-6}$ s^{-1}). The uniform quality of our materials has been controlled by the Brinnel hardness test (HB = 190), and microscopic observations were made for the ferritic structure.

b) The bonding was performed with an epoxy adhesive, polymerized at room temperature, EPONAL 317 (Registered mark of CECA, France). Traction tests, effected on specimens made in bulk adhesive, gave $E = 5800$ MPa, $\nu = 0.327$. The traction curves ($\dot{\varepsilon} = 10^{-6}$ s^{-1}) showed an elastic, brittle behaviour.

c) To increase the strength of the bond between the adhesive and the adherends, these were sandblasted with corundum particles, of mean diameter equal to 169 μm. The study of the surface state, developed by Gilibert,[1] has shown that this yields a roughness adapted to the mean diameter of the mineral

fillers contained in the adhesive ($d_m = 7\ \mu m$).[1,6,9] Their roughness was defined by the NF-E05-015 criteria (French automobile standards).

The study of the influence of the thickness of the adhesive layer, with sandblasted adherends (thickness $e_s = 4.5$ mm), always showed an internal fracture due to shear (in the case of steel of French standards XC18 and XC90, for $0.05 < e_j < 1.5$ mm).

Figure 1 describes a test specimen whose dimensions virtually maximize the breaking force. We used this model to study the influence of the bevelling (or scarfing) of the ends of the adherends T_1 and T_2 (Figure 2), on the mechanical behaviour in shear, under traction.

2.2 Bevelled double-lap

The specimen is described in Figure 2. It comes from the same materials as the unbevelled double-lap, shown in Figure 1. The design and manufacture of the test specimens presented many technical problems, due to the difficulties that we had in handling some of the steel sheets with ends bevelled at only a few degrees. In particular, we studied, designed and developed devices that allowed the adherends to be assembled very accurately during the polymerization of the adhesive joint.

2.3 Experimental method

2.3.1 *Preliminary statements* The detection system by electrical strain gauges, that we have developed,[1] localizes:

a) the regions of microcrack initiation, and

b) the area where the debonding of the sheets (or of the core) occurs, in the case of adhesive failure.

The slope inversions (Figure 3) show that, at the corresponding points (situated towards the free edge of outer adherends):

– The steel sheets do not lengthen any more, but contract,

– The tensile load is no longer transmitted in the same way to the steel sheets through the adhesive joint.

Therefore, locally there occurs:

– either an adhesive failure in the interface resin–steel, on the side of T_1 and T_2 or on the side of the core A.

– or a shear fracture of the joint J.

The examination of the pieces after fracture determines the type of the fracture.

2.3.2 *Various types of fracture observed* Depending on operating conditions and on the geometrical and mechanical parameters of the test specimen, various

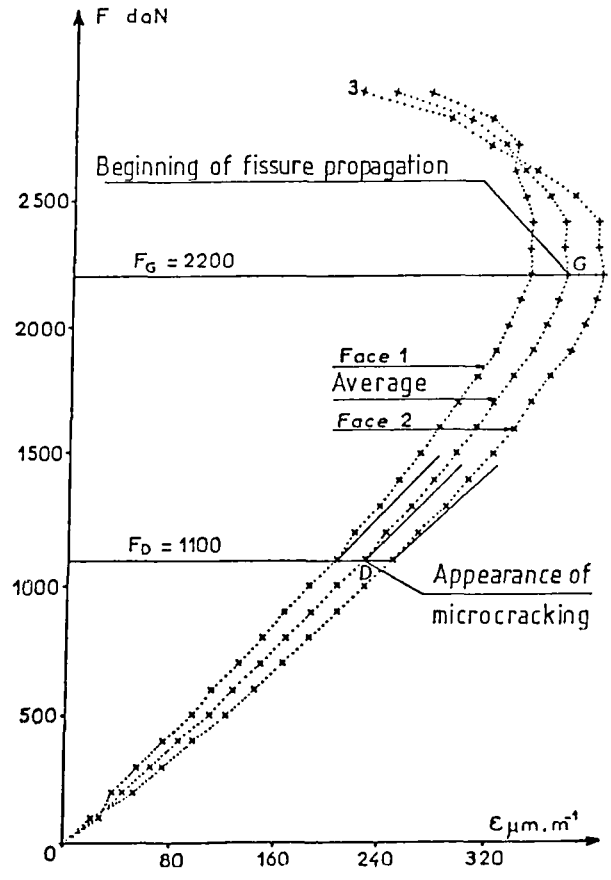

FIGURE 3 Graphic determination of the loads, beyond which the microcracks occur, and the flaws extend, in the case where the adherends have a sand blasted surface state.

types of fractures may occur:

a) Shear fracture of the joint.

When the total failure of the specimen was due to a shear fracture of the joint, one part of the adhesive stuck to the core surfaces, and the other part to the sheet surface. The general debonding happened only by the failure of the resin macro-molecules that composed the adhesive joint. For this type of chemical bonding, we used the symbol (J–J). (See the observation of the surfaces after fracture of the samples.[1])

b) Adhesive failure.

Its main features are the debonding of the joint at the resin-core or resin-sheet interfaces. All the adhesive is removed from one of the adherend surfaces, the core or the steel sheets, therefore the bonds between resin and metal, respectively, referred to by (J–T) and (J–A), are destroyed under the stress generated by the tensile load. Thus, in the parts of the joint where this type of

fracture occurs, the bonds (J–T) or (J–A) are less strong than (J–J) for the regarded load.[1,7]

An experimental study for this type of bond has been presented by Komiha,[10] for which the author has carried out all the tests studied. A thorough study of this type of bond brings to light the early initiation of microcracks at the resin/aluminium alloy interface. Experimentation has defined the basis of an analytic model to adapt continuum mechanics to this type of mechanical behaviour.[11]

c) Mixed fracture.

The two types of debonding previously described can coexist in the same test specimen. The predominance of one or the other depends on the surface state of the adherends and on geometrical and mechanical parameters.

2.3.3 *Choice of the graphic representation* We can draw the following types of curves:

– load F according to the microstrain registered for particular abscissa, *i.e.* $F = f(\varepsilon)$ (curve type 1, Figure 3).

– registered microstrain ε according to the position of the gauge for various given loads, *i.e.* $\varepsilon = f(x)$ (curve type 2, see volume II of Reference 1).

– load F according to the calculated stress in a particular abscissa, *i.e.* $F = f(\sigma)$ (curve type 3, see volume II of Reference 1).

– calculated stresses σ according to the abscissa along the sheets, *i.e.* $\sigma = f(x)$ (curve type 4, see volume II of Reference 1).

To study the phenomena more thoroughly, it is interesting to draw these curves for each face and each type of value (longitudinal or transverse). We can also draw[1,12] the average curves defined by symmetrical abscissas with respect to the longitudinal axis O'X' of the main reference mark (Figure 1), and it should be noted that they are representative of the behaviour of the joint.[1]

The utilization of the recorded, or calculated values, often demands:

– the choice of the scales best adapted to the representation of the phenomena.

– the reproducibility and the comparison between several experiments.

– the setting apart, and the enlargement, in a specific region, of parts of the curves that show clearly the characteristic properties.

We developed programs to carry out all this work automatically.

3 STUDY OF THE PREFERENTIAL SHEARING OF THE ADHESIVE JOINT J.

Considering sand-blasted surface states, the fracture of the test-specimen is a preferential shear fracture inside the joint. In order better to analyse the phenomenon in this case, we need to consider the average curves 1 (F_{D_1}, F_{G_1}),

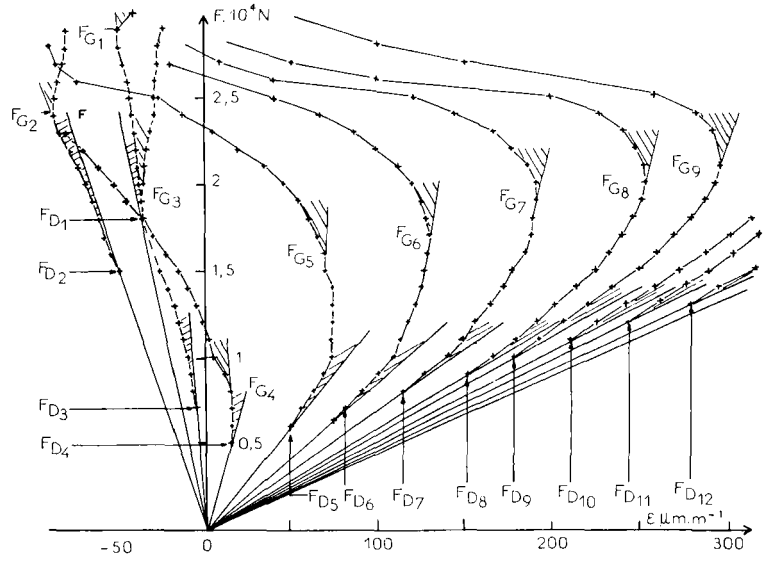

FIGURE 4.1 Mechanical behaviour of the free ends of sheets T_1 and T_2. Variation of the microstrains, as a function of the gauges' position, and of the pulling effort.

$2(F_{D_2}, F_{G_2}), \ldots, 30\ (F_{D_{30}}, F_{G_{30}})$ (Figures 4.1 and 4.2, and Table I), corresponding to gauges $I_1, \ldots, I_{30}$, and to their symmetrical figures, whose respective distances x from the center to the free edge of the overlaps are shown in Table I.

When the tensile load increases from 0 to 3000 daN (ultimate breaking load), gauges 1 to 30 indicate that there is a linear elastic behaviour, up to the microcrack initiation thresholds F_{D_n} $(n = 1, 2, \ldots, 30)$.

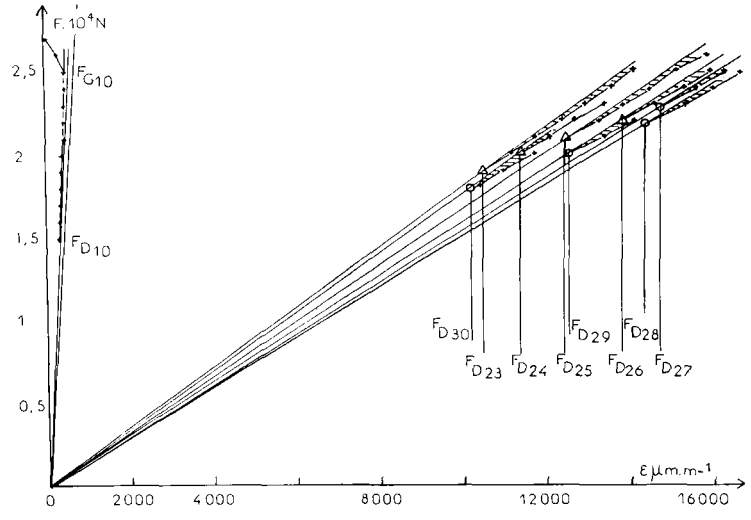

FIGURE 4.2 Mechanical behaviour of the loaded end of sheets T_1 and T_2. Variation of the microstrains, as a function of the gauges' position, and of the pulling effort.

TABLE I
Evaluation, at different abscissas, of the local thresholds, corresponding, respectively, to microcrack initiation and to flaw propagation

gauge No.	1	2	3	4	5	6	7	8	9	10
x mm	1.5	3.5	5.5	7	9.76	11.76	13.76	15.76	17.76	19.76
F_D daN	1800	1500	700	500	600	700	800	900	1000	1100
F_G daN	2900	2400	1800	800	1600	1700	1900	2000	2100	2200
gauge No.	11	12	23	24	25	26	27	28	29	30
x mm	21.76	23.76	80.20	81.20	82.20	83.20	84.20	85.20	86.20	87.20
F_D daN	1200	2300	1900	2000	2100	2200	2300	2200	2200	1800
F_G daN	1400	2400	F_R	F_R	F_R	F_R	F_R	F_R	F_R	F_R

For $F_{D_4} = 500$ daN and $x = 6.7$ mm, we observe the initiation of the first microcracks, which occur inside the joint under the shear stress,[3,6,13,14,15] close to the free ends of T_1 and T_2. When the load increases further, the microcracks extend gradually towards the free ends of the steel sheets, and more quickly towards the center of the overlap. Only for $F = 1700$ daN ($x = 70.5$ mm) do they appear close to the other end ($x = 88$ mm). Beyond 1700 daN they develop very slowly to the right and much more quickly to the left. Finally above 1800 daN, microcracks appear at the end (abscissa $x = 87.2$ mm), due to the predominance of the normal stresses of tearing.[16]

Figure 5 indicates that when F reaches 2800 daN, the microcracks extend along the whole joint. Gauge 1 is situated at 1.5 mm from the free end of the steel sheet T_1; our study continues in the area limited by $0 < x < 1.5$ mm.

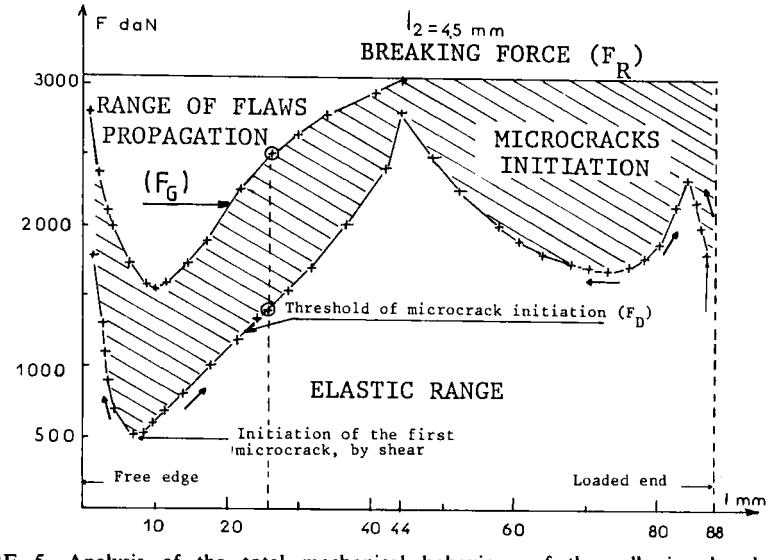

FIGURE 5 Analysis of the total mechanical behaviour of the adhesive bonded structure. Determination of the elastic area, of the area of microcrack initiation in the stable state and of the area of unstable extension, near total failure.

Then we shall be able to specify the complex mechanical behaviour of the specimen in its angular parts.

The grey surface (Figure 5) represents the area in which microcracking gradually takes place and microcracks develop up to their critical size (see curve F_{G_n}). From (F_{G_n}), they meet and develop cracks, which propagate more rapidly as the value of the load approaches the ultimate value ($F_R = 3000$ daN). Therefore, it turns out that the two ends of the bonded structure do not behave in the same way under the strain (see Chap. VIII, Fig. VIII. 9 of Reference 1).

In his earlier work,[1] one of the authors had not presented the detailed work carried out with the help of the tested metals, especially those related to low carbon steel, with 0.18% and 0.90% carbon (see Chap. XIII. 4.2, tables XIII.1 and XIII.2 of Reference 1). Indeed, within the limits of that research, it was necessary to give a global interpretation, in correlation with all the tested samples. The strain-gauge located at the abscissa $x = 25.5$ mm, corresponding to $X' = 84.5$ mm (Figure 1), showed that the first microcracks usually take place in a shear mode, in the neighbourhood of the ends (for the tested cases).

This work represents an experimental analysis that is very delicate, very expensive and time consuming to develop, but it enabled us to get closer to the real behaviour of the tested structure. At the same time, we developed better-adapted analytic calculations[3,5,7,10,13–22] and numerical (finite element) methods.[3,23] We also tried to analyze the mechanical behaviour of the joint with the help of an acoustic method.[24] The first results are encouraging and a precise comparison is being carried out.

The threshold for microcrack initiation, obtained by this method, is confirmed by the first indication of acoustic activity of the joint using DUNEGAN detectors[25] (Work supported by the French Ministry of Defence under contract DRET No. 1054).

4 EXPERIMENTAL STUDY OF THE BEVELLED DOUBLE-LAP

The bevels are characterized by their length l_2 (Figure 2), thus the angle α of the tapered side is defined by $\sin \alpha = e_s/l_2$ (e_s: thickness of the sheets T_1 and T_2, at their loaded end).

The length varied between the two limit values $l_2 = 4.5$ (UBDL, $\alpha = 90°$) and $l_2 = 88.3$ mm, which corresponds to the bevelling of the sheets all along the overlap ($l = 88$ mm and $\text{tg}\ \alpha = e_s/l$). The research, in progress, will enable us to specify the mechanical behaviour of such a joint for angles larger than 90° and for cores bevelled at their end (the extremity fixed to the loaded side of the sheets T_1 and T_2). In the present work we are studying the mechanical behaviour of the bevelled double-lap when the angle α is acute.

Figure 6 and Table II concern the structure described in Figure 2 with the same overlap length ($l = 88$ mm), the same adhesive (EPONAL 317), the same adherend material (XC 18), the same surface state ($R_t = 7\ \mu$m), and the same experimental conditions; this joint has the maximum breaking strength ($F_R =$

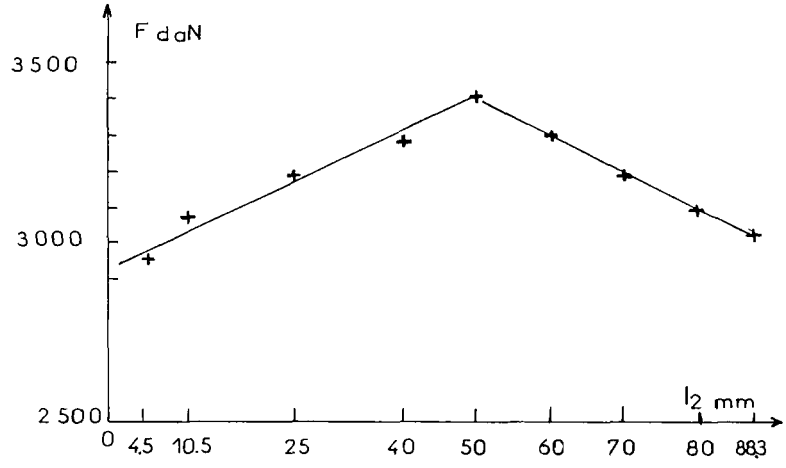

FIGURE 6 Determination of the ultimate failure, for nine values of the bevel length between 4.5 mm and 88 mm.

3500 daN) for the optimal value $l_2 = 50$ mm. Its strength is minimum for $l_2 = 4.5$ mm ($\alpha = 90°$, UBDL, $F_R = 2950$ daN).

The experimental study in the neighbourhood of the ends has only been refined for the two values $l_2 = 4.5$ mm ($\alpha = 90°$) and $l_2 = 10.5$ mm (in the case of the chamfer generally done to lessen the highest shear stress near the free side of the junction-plate). We observe (see Figure 7) that the chamfer generates a very early initiation of microcracks ($F_D = 200$ daN) but gives such a state of stress to the end of the joint that the crack extends only very slowly towards the free ends of the tapered sides T_1 and T_2. At the other extremity, this initiation occurs much later ($F_D = 2000$ daN, $x = 66$ mm) than for the unbevelled double-lap (Figure 5, $\alpha = 90°$, $F_D = 1700$ daN, $x = 70.5$ mm). Finally, as a result, there is a significant increase of the mechanical strength. Indeed, the curve showing the beginning of

TABLE II
Overall view of the main experiments

No.	l_2	Trial No./F_R(daN)				Average
D.R.B.	mm	1	2	3	4	$\bar{F}_R$
1	4.5	2900*	2900*	3000*	3000*	2950
2	10.5	3100	3000*	3100	—	3066
3	25	3200	3150	—	—	3175
4	40	3250*	3300	—	—	3275
5	50	3450	3350	3400*	3400*	3400
6	60	3300	—	—	—	3300
7	70	3230	3150*	—	—	3190
8	80	3100	—	—	—	3100
9	88.3	3000*	3100*	3050	—	3050

* Trials referred to by the symbol (*) correspond to test specimens equipped with electrical strain gauges.

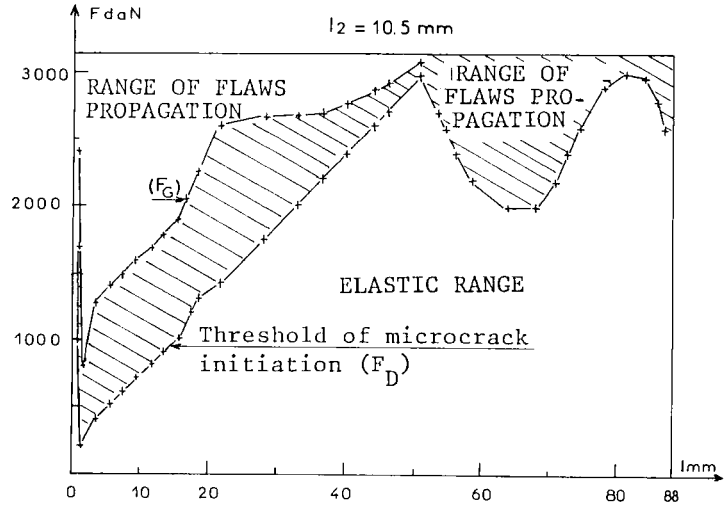

FIGURE 7 Analysis of the total mechanical behaviour of the adhesive bonded bevelled structure for $l_2 = 10.5$ mm (analogous to Figure 5).

the crack extensions (F_G) indicates that these begin later at total scale, and develop along most of the length of the overlap.

Generally speaking, the effect of the decrease of α is to emphasize this trend, up to the optimal value of l_2 ($l_2 = 50$ mm, Figure 8).

Thus, the part of the area entitled "Range of Microcracks Initiation," in Figures 5, 7, 8 and 9, and located on the side of the free edge of the outer

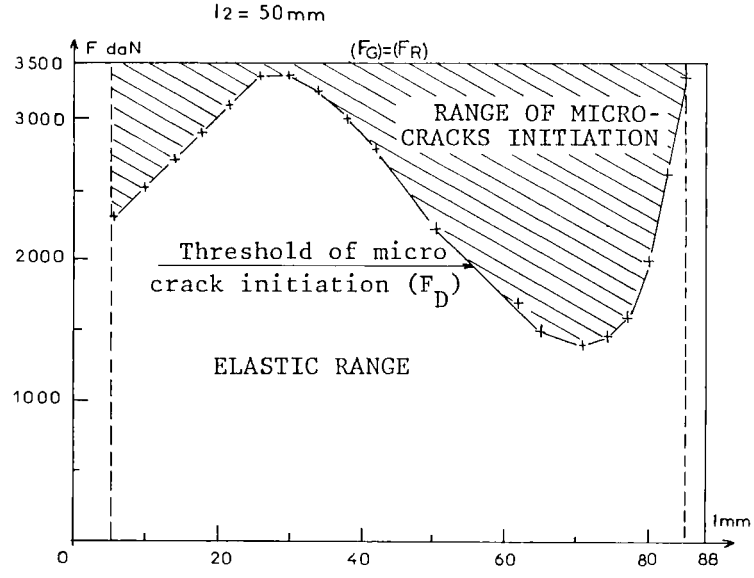

FIGURE 8 Analysis of the total mechanical behaviour of the adhesive bonded bevelled structure for $l_2 = 50$ mm. (analogous to Figure 5).

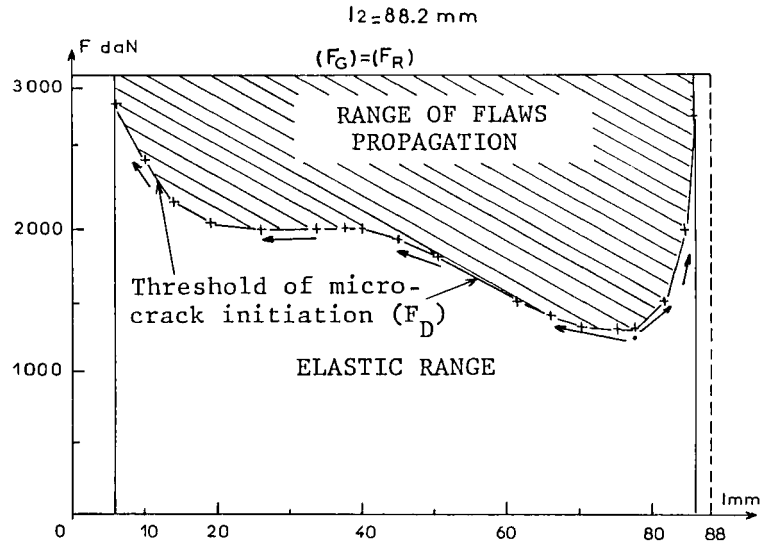

FIGURE 9 Analysis of the total mechanical behaviour of the adhesive bonded bevelled structure for $l_2 = 88$ mm. (analogous to Figure 5).

adherends, where the microcracks begin early in the case of the UBDL, shrinks progressively when l_2 goes up from 4.5 mm (UBDL) to 50 mm. We no longer observe the same curves $F = f(\varepsilon)$ as those represented in Figure 4.2 (change of sign of $df/d\varepsilon$ for F_G). As a result, the behaviour of the specimen becomes elastic up to the neighbourhood of rupture ($F_G = F_R$).

The initiation threshold of the first microcracks, for the optimized structure ($l_2 = 50$ mm), is situated opposite the free edge of the sheets ($F_D = 1400$ daN, $x = 70$ mm); they appear much later near the vertex of the tapered sides ($F_D = 2300$ daN, $x = 6$ mm). When $l_2 = 50$ mm and for $0 < x < 6$ mm, our first observations seem to confirm that the extremity of the bevel adapts to the strains that probably quickly become significant in those end areas.

Finally, when l_2 increases beyond the optimal value, the breaking strength of the model decreases and the first microcracks continue to appear near the free end of the core A, but occur progressively in the central part at a lower threshold (Figure 9). As a result, there is a reduction of the strength of the specimen undergoing shear, by means of a traction force.

5 CLASSICAL THEORY

The classical theory corresponds to the hypothesis of loading in simple traction of the adherends (Figure 10). It is valid only in the assumption of very thin adherends. For a simplified calculation, we only consider the case when the bevel

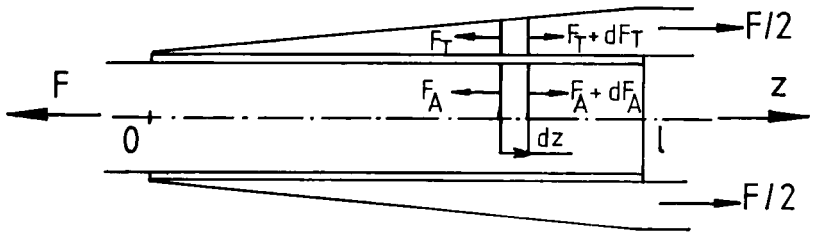

FIGURE 10 Approximation of the classical theory.

edge extends over the total length of the overlap, that been described by Adams *et al.*[24]

Simplified solution, in the linear domain The relationships used for the calculation are

$$y = 0 \text{ for } \zeta = 0; \qquad y = 1 \text{ for } \zeta = 1 \tag{1}$$

$$\tau/\tau_m = \psi/\psi_m = dy/d\zeta \tag{2}$$

$$\Phi = (\varepsilon_s/\zeta + \varepsilon_A) \cdot y - \varepsilon_A \tag{3}$$

where the symbols are as given later. In the linear domain, if the singularities are neglected, we can use a regular expansion for y, *e.g.* of third order:

$$y = y_1\zeta + y_2\zeta^2/2 + y_3\zeta^3/3 \tag{4}$$

and we express ψ in two different ways, on the one hand with (2) and (4), and on the other hand with the integration of relationship (3). By matching the two results, we obtain two linear equations between y_1, y_2, and y_3; a third equation results from condition (1) at $\zeta = 1$. The expression of the solution y_1, y_2, and y_3 simplifies when α^2 and β^2 are large with respect to unity, so that the y expression is:

$$y = r\zeta - r^2\zeta^2 + (1 - r + r^2)\zeta^3 \tag{5}$$

The calculated microstrains ε_L are compared with the experimental values in Figure 11.

Shear modulus evaluation of the joint Experimental ε_L values furnish y by the relationship:

$$y = \varepsilon_L \cdot \zeta/\varepsilon_s \tag{6}$$

so that Equation (2) is used to evaluate τ at the midpoint between two successive strain gauges. On the other hand, expression (3) of Φ is integrated stepwise, starting from a definite strain gauge location, where ψ is equal, say, to ψ_0; accordingly, the following formula furnishes $\hat{\psi}_0$ (*i.e.* $\psi - \psi_0$), also at the

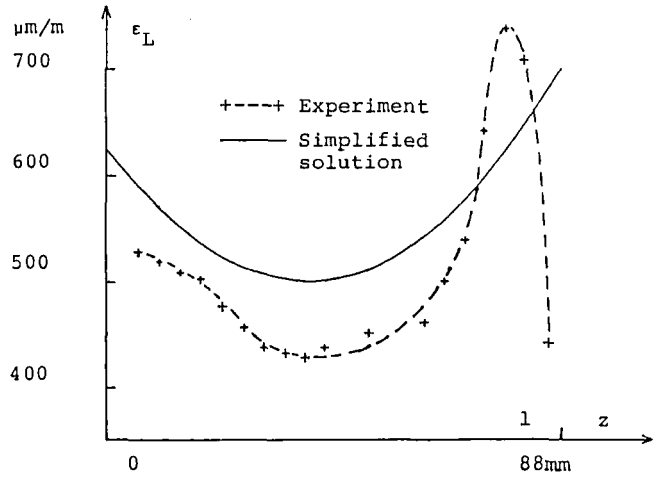

FIGURE 11 Comparison of the microstrain profiles, when the bevelling is realized over the total length of the outer adherends.

mid-points of the intervals:

$$\hat{\psi}(t) = t\left\{\Phi_2 + t\left[\frac{\Phi_1 - \Phi_2}{h_1(h_1+h_2)}\left(\frac{t}{3} - \frac{h_2}{2}\right) + \frac{\Phi_3 - \Phi_2}{h_2(h_1+h_2)}\left(\frac{t}{3} + \frac{h_1}{2}\right)\right]\right\} + \hat{\psi}_2 \qquad (7)$$

Now, τ and $\hat{\psi}$ are related by:

$$\tau = G(\hat{\psi} + \psi_0)/e_J \qquad (8)$$

and the least-squares method yields the evaluation of G/e_J. The calculation has been done for $F = F_D = 1300$ daN (microcrack initiation). In order to obtain a meaningful result, it was necessary to discard the two gauges located near the loaded end of the sheets (at $z = 81.5$ mm and 85.5 mm, respectively). Then the result, $G = 2204$ MPa, is close to the linear value of 2185 MPa, deduced from the measurements of E and ν on bulk adhesive.

CONCLUSIONS

Our study shows that the mechanical behaviour of a symmetrical double-lap adhesive structure is very complex. The knowledge of the initiation threshold of the first microcracks in a composite or bonded sample provides significant information. The lifetime of the structure depends on its initial properties, and it is essential to determine very carefully the beginning of the damage under a simple static load, in order to study its evolution, in the elastic range or in its neighbourhood, when the load becomes more complex (fatigue, shocks, etc. . .), and environmental conditions become more severe (pressure, temperature, humidity, etc. . .). The experimental study, relative to the bevelled double-lap, enables us to show that there is an optimal value of l_2, that gives maximum

strength to the specimen. It also brings to the fore the mechanism of the initiation and extension of microcracks in the adhesive joint. Its brittleness is correlated with the angle α of the bevel. Therefore, this work can be taken as a starting point, in order to establish a model for the observed phenomena.

Generally, speaking, this type of research can be achieved only if there is very close collaboration between the experimentalist and the theoretician.

This analysis shows that the classical theory is not exact near the loaded end of the sheets. In this region, the microstrain profile displays a superficial dilatation, as for the non-bevelled joint; in the latter case, experimental characterization and interpretation takes into account the flexure of the outer adherends as, for example, in the model developed by the authors.[26–29]

The present study shows also that the scarfing of the outer adherends can increase the threshold of microcrack initiation. This fact is probably significant in fatigue behaviour, where the quality of the joint is paramount. In this respect, the evaluation method of the shear modulus of the joint yields an estimate that is in good agreement with the bulk properties of the adhesive.[11,30–33]

In conclusion, it might be advisable to perfect simultaneously the equations and the method of solution in order to obtain a better experimental and theoretical fit between the microstrain profiles along the overlap.

The experimentation and the computation are delicate. They demand long and tedious researches that require long shared experience. When the results are found, they may be programmed quickly and easily on a micro-computer.

Acknowledgements

We gratefully acknowledge the financial support of the French Ministry of Research and Industry, and the Group ARMINES–TRANSVALOR (60, Boulevard Saint-Michel, 75272 Paris Cedex 06), for the development of this research: French Patent no. 8614137-1986, Owner: ARMINES, Inventor: Y. Gilibert, and European Patent no. 87402264.3.-1987.

We also wish to thank the French Ministry of Defence for granting the DRET Contract no. 87.236.

SYMBOLS USED

l_2 = length of the sloping edge, shown in Figure 2, for a bevel angle varying from 90 degrees to a few degrees

e_s = thickness of the non-scarfed sheets (at their loaded end)

E_T, ν_T = Young modulus and Poisson ratio, of the sheets

E_A, ν_A = Young modulus and Poisson ratio, of the core

E, ν = Young modulus and Poisson ratio, of bulk adhesive

$\dot{\varepsilon}$ = strain rate utilized in the tensile test of the materials

d_m = mean diameter of the mineral fillers in the adhesive

l = total length of the overlap

r = $e_s \cdot E_T/(e_A \cdot E_A)$

z or x = longitudinal abscissa, varying from 0 (free edge of the bevelling) to l (loaded end of the sheets)

x' $= l/2 - x$
X' = abscissa corresponding the reference mark in Figure 1
F = traction force
F_D = threshold traction for microcrack initiation
F_G = threshold force for flaw propagation
F_R = traction force for complete fracture
F_T = longitudinal force in each sheet (local value)
F_A = half longitudinal force in the core (local value)
y $= F_T/(F/2)$ dimensionless traction in the sheets
ζ $= z/l$ dimensionless abscissa
l_1 = width of the test specimen
τ = local longitudinal shear stress along the joint
τ_m $= F/(2l \cdot l_1)$ mean shear stress along the joint
G = shear modulus of the adhesive
α^2 $= \varepsilon_s l/\psi_m$; $\beta^2 = \varepsilon_A \cdot l/\psi_m$
e_J = thickness of the joint
ψ = relative longitudinal displacement between the adherends
ψ_m $= \tau_m e_J/G$ mean value of ψ along the overlap
Φ $= d\psi/dz$ derivative of ψ with respect to z
ε_A $= F/(2e_{A/2} \cdot E_A \cdot l_1)$ longitudinal strain in the core at $z = 0$
ε_L $= F_T/(e_T E_T l_1)$ microstrain along the sheets (local value)
ε_s $= F/(2e_s E_T \cdot l_1)$ sheets microstrain at $z = 1$
ψ_0, z_0 = values at some particular strain gauge,
$\hat{\psi}$ $= \psi - \psi_0$
t $= z - z_2$ local abscissa, used in equation (7)

Subscripts 1, 2, 3, in equation (7) index three successive gauges

h_1 $= z_2 - z_1$ and $h_2 = z_3 - z_2$ in equation (7)
e_A, e_T = thickness of core, and sheets (local values)

References

1. (a) Y. Gilibert, *Contribution à l'étude de l'adhésivité de matériaux collés par l'intermédiaire de résines époxydiques.* Thèse de Doctorat d'Etat ès Sciences Physiques, Université de Reims, 1978; (b) Y. Gilibert, *Contribution à l'étude de l'adhésivité de matériaux collés par l'intermédiaire de résines époxydiques*—Rapport de Recherche ENSTA, no. 180, Janvier 1984.
2. J. Bernasconi and Y. Gilibert, *Méthode de tracé automatique des courbes de déformations et de contraintes engendrées à la surface d'éprouvettes de traction réalisées en acier ou en béton plaqué*—Note de recherche E.N.S.T.A., no. 053, Décembre 1983.
3. E.N.S.T.A./E.N.S.M.S.E./ARMINES—*Recherche de l'amélioration des assemblages collés sollicités à la traction*—M.R.I. Décision d'aide no. 82 S 0962 du 25 Novembre 1982 (travaux en cours), Laboratoire de Mécanique et Energétique, Groupe "Composites et Collage", 91120 PALAISEAU, et Ecole des Mines de Saint-Etienne.
4. E. Chevestrier and Y. Gilibert, T.A.E.P., Techniques Avancées, Etudes et Projets JUNIOR ENTREPRISE, E.N.S.T.A., 32, Boulevard Victor, 75015 Paris. *Adaptation d'une méthode de tracé automatique des courbes de déformations et de constraints engendrées à la surface de composites plans collés sur micro-ordinateur (Tektronix et H.P.)*—E.N.S.T.A., L.M.E., Groupe Composites et Collage, Juillet-Août 1984, Rapport interne T.A.E.P./E.N.S.T.A./L.M.E./G.C.C.

5. Y. Gilibert and A. Rigolot, "Théorie élastique des assemblages collés à double recouvrement"—*Quatrième Congrès Français de Mécanique,* pp. 301–302, Nancy, 1979.
6. Y. Gilibert and G. Verchery, in *ADHESIVE JOINTS: Formation, Characteristics and Testing* K. L. Mittal, Ed. (Plenum Publishing Corporation, New York, 1984), pp. 69–84.
7. Y. Gilibert and G. Verchery, *Mise au point d'adhésifs hautes performances pour applications en aéronautique, électronique et mécanique*—Rapport fin de contrat D.G.R.S.T., REF. IRCHA D.6456 (Décision d'aide no. 81 P1 365 du 21 Juillet 1981). Partie E.N.S.T.A.: REF. ENSTA—YG/Sm, ARMINES, 1984. (partie "IRCHA" par A. M. Fournier, E. Morel, D. Boulonnais, REF C 70-DB/JC).
8. M. Khadhraoui-Lattreche, *Etude de l'endommagement des composites Graphite/Epoxy soumis à des chargements quasi-statiques répétés en cisaillement*—Thèse de docteur-ingénieur. I.N.S.T.N., E.N.S.T.A./L.M.E./G.C.C., 1984.
9. Y. Gilibert and Verchery, see Reference 6.
10. M. A. Komiha, *Analyse théorique et expérimentale de l'influence de l'épaisseur du film de colle, dans un assemblage collé, à double recouvrement,* Doctorat du 3ème cycle, Paris 6—ENSTA/LME/GSC, 1983.
11. (a) Y. Gilibert, M. L. L. Klein and A. Rigolot, *Modélisation d'un composite plan en présence de microdéfauts,* Rapport de recherche E.N.S.T.A./L.M.E./Groupe Composites et Collage, no. 207, Mars 1986; Paris. (b) Y. Gilibert, M. L. L. Klein and A. Rigolot, *Composites, no. 3,* Mai-Juin 1986, pp. 221–229, Paris.
12. Y. Gilibert, H. Miller and G. Gautron, *Annales Université A.R.E.R.S.,* Reims 1976, T. 14, pp. 17–27.
13. A. Rigolot, "Application de la méthode des développements asymptotiques raccordés au calcul des effets d'extrémités dans un composite plan collé"—*2ème Congrés International du GAMNI,* du 2 au 7 Décembre, pp. 245–259, 1980, France.
14. Y. Gilibert, M. A. Komiha A. Rigolot and G. Verchery, "Analyse théorique et expérimentale, de l'influence de l'épaisseur du film de colle, dans un assemblage collé à double recouvrement"—Communication présentée à l'occasion des Journées Universitaires de Génie Civil 26 et 27 Avril 1984, E.N.S.E.T. Cachan. *Publication Universitaire de Génie Civil (C.R. de l'A.U.G.C. 1984).*
15. Y. Gilibert, M. A. Komiha and A. Rigolot, *Théorie élastique de l'assemblage collé à double recouvrement: utilisation de la méthode de développements asymptotiques raccordés au voisinage des extrémités.* Rapport de Recherche E.N.S.T.A., no. 189, 65 pages, Juillet 1984.
16. A. Gilibert, M. A. Komiha and A. Rigolot, *Annales de l'I.T.B.T.P.,* no. 425, série: théories et méthodes de calcul, pp. 50–67, 1984, Paris.
17. A. Rigolot, *Sur une théorie asymptotique des poutres droites*—Thèse de Doctorat d'Etat ès Sciences Mathématiques, Université de Paris **6,** 1976.
18. Y. Gilibert and A. Rigolot, *Journal de Mécanique Théorique et Appliquée* **3,** 341–372 (1978).
19. Y. Gilibert and A. Rigolot, *Compte Rendus de l'Académie des Sciences de Paris, Mécanique des Solides, Série B* **288,** 387–390 (1979).
20. Y. Gilibert and A. Rigolot, *Annales de l'I.T.B.T.P.,* no. 408, série: théories et méthodes de calcul, p. 255, 1982, France.
21. A. Rigolot—*Journal de Mécanique Théorique et Appliquée* **1,** 799–839 (1982).
22. Y. Gilibert and A. Rigolot, Conception optimale des composites plans collés: analyse expérimentale et modélisation de la "dissymétrie" des contraintes aux extrémités d'un assemblage balancé. *A.M.A.C. "Le calcul des structures en matériaux composites",* Saint-Etienne, 15 Novembre 1984.
23. Le Monet, *Analyse du rapport Causse*—Dossier d'option Matériaux, 2ème année, Ecole Nationale Supérieure des Mines de Saint-Etienne, effectué sous la responsabilité de Y. Gilibert.
24. R. D. Adams, S. H. Chambers, P. J. A. Del Stroher and N. A. Peppiat, *J. Strain Analysis* **8,** 52–57 (1973).
25. I.R.C.H.A., Service Matériaux Plastiques, Centre de Recherche, 91710 Vert-Le-Petit.
26. Y. Gilibert, M. L. L. Klein and P. Bougard, *Composites, no. 3,* Mai-Juin 1987, pp. 12–21, Paris.
27. Y. Gilibert and M. L. L. Klein, Study of Double-Lap Adhesive-Bonded Joints, in the Neighbourhood of their Extremities. *Euromech Colloquium 227, Mechanical Behaviour of Adhesive Joints,* G. Verchery and A. H. Cardon, (Ed.) (Editions Pluralis, Paris, 1987), pp. 469–478.
28. Y. Gilibert, M. L. L. Klein and A. Rigolot, *Revue de Métallurgie,* Paris, no. 9, September 1987, p. 100.
29. Y. Gilibert, M. L. L. Klein and A. Rigolot, in *Combining Materials: Design, Production and Properties,* **2,** J. C. Maso, Ed. (Chapman and Hall, London, New York, 1987), pp. 895–902.

30. M. L. L. Klein, Y. Gilibert and A. Rigolot, "Interprétation des profils de contrainte mesurée le long de l'assemblage à double recouvrement sollicité en traction", *Première Semaine Internationale de l'Adhésion et de l'Assemblage-ADHECOM*, Bordeaux, France, 1986.
31. Y. Gilibert, M. L. L. Klein and A. Rigolot, *Matériaux et techniques* **75**, 29–36 (1987).
32. Y. Gilibert, M. L. L. Klein and A. Rigolot, *Adhesively Bonded Joints: Testing, Analysis and Design*, W. S. Johnson, Ed. *ASTM STP 981* (ASTM, Philadelphia, 1988), pp. 39–53.
33. Y. Gilibert, M. L. L. Klein and A. Rigolot, "Shear modulus estimation of the adhesive in a double-lap bonded joint". *Preprints of ICM5 Conference* (Fifth International Conference on Mechanical Behaviour of Materials, Beijing, China, June 3–6, 1987) (Pergamon Press, United Kingdom).
34. J. P. Causse, Les matériaux—*Rapport au Ministre de la Recherche et de l'Industrie*—30 Juin 1982, France.
35. Y. Gilibert, *L'Usine Nouvelle*—no. 28, 14 Juillet 1983, participation à un dossier réalisé par D. Coué, pp. 36–42.
36. (a) Y. Gilibert, "Etude de l'influence du biseautage des extrémités des substrats sur le comportement mécanique d'un composite plan collé, sollicité à l'essai de cisaillement par traction" *–19ème Colloque National Annuel, Rhéologie des Matériaux Anisotropes*, Paris, France, 1984; (b) Y. Gilibert and A. Rigolot, Rapport de Recherche ENSTA/LME/GCC no. 196, Janvier 1985; (c) Y. Gilibert, Contrat de Recherche, ARMINES/MRI/ENSTA, no. 82S0962 du 18 novembre 1982; (d) Y. Gilibert, "Analyse expérimentale du comportement mécanique fin des joints collés poxydiques d'assemblages à double recouvrement biseautés" *Preprints of CANCAM 87: 11th Canadian Congress of Applied Mechanics*, The University of Alberta, Edmonton, Canada, May 31–June 4, 1987.
37. Y. Gilibert, A. Le Méhauté and G. Verchery, *Etude d'un capteur électrochimique de rugosité*—Action concertée capteur—M.R.I. Décision no. 83 T 0610, 27 Septebre 1983 (C.G.E. Marcoussis/E.N.S.T.A. Palaiseau/ARMINES Paris).
38. O. Pierret, *Les traitements de surface mécaniques et chimiques pour le collage des toles en alliages légers dans la construction aéronautique*—Dossier d'option Matériaux, 2ème année, Ecole Nationale Supérieure des Mines de Saint-Etienne, effectué sous la responsabilité de Y. Gilibert.
39. C. Phang, J. F. Lerooy and P. Goubault, *Poutres stratifiées et collées en flexion*—Rapport de projet d'enseignement par la recherche, sous la responsabilité de Y. Gilibert et G. Verchery, Laboratoire de Mécanique et Energétique, Groupe G.S.C., ENSTA Palaiseau, 1982.
40. M.S.M.R. El Shaikh, *Modélisation, calcul et identification du comportement mécanique de structures composites et sandwiches*—Thèse de Doctorat d'Etat ès Sciences Physiques, Université de Paris VI/ENSTA/LME/GCC, 1984.
41. V. Saubestre and D. Pierre, *Etude mécanique d'un ski de fond. Analyse des déformations et des constraintes.* Option C2 "Tenue des structures", Ecole Polytechnique, 91128 Palaiseau Cedex.—Rapport de stage d'option, effectué sous la Direction de G. Verchery et Y. Gilibert (partie expérimentale) à l'E.N.S.T.A. de Mars à Juillet 1982.
42. (a) Y. Gilibert and A. Rigolot, Analyse théorique et expérimentale de l'assemblage par collage de tubes métalliques. *Compte Rendus du 20ème Colloque du Groupe Français de Rhéologie*, du 27 au 29 Novembre, Paris, 1985, pp. 332–346; (b) Y. Gilibert and A. Rigolot, *Analyse théorique et expérimentale de l'assemblage par collage du tubes métalliques.* Rapport de Recherche E.N.S.T.A., no. 199, 41 pages, Avril 1985.
43. A. Rigolot, Régularisation de l'effet Saint-Venant dans une structure plane, composite, collée, soumise à des sollicitations de traction. *Euromech Colloquium: The inclusion of local effects in the analysis of structures*—Sept. 11–14 1984, Cachan, France.
44. Y. Gilibert and A. Rigolot, *Mechanics Research Communications*, **8**, 269–274 (1981).
45. D. Vokersen, *Construction métallique*, no. 4, pp. 3–13, 1965.
46. Y. Gilibert, *et al., R.I.L.E.M. Matériaux et Constructions*—Vol. 9, no. 54, pp. 419–423, 1976.
47. Y. Gilibert, *et al., Analyse expérimentale et théorique des assemblages collés du type double recouvrement et du type simple recouvrement en sifflet*, Rapport de recherche no. 212, E.N.S.T.A./L.M.E./Groupe Composites et Collage, Janvier 1987, Paris.
48. J. P. Charles and Ph. Jeannin, *Rapport enseignement par la recherche* (élèves de 3ème année, E.N.S.T.A./L.M.E./G.C.C., 1984–1985).
49. Y. Gilibert and A. Rigolot, "Calcul et mesure des contraintes dans les assemblages composites collés." Communication présentée à la *Journée Régionale*: "*Science et Défense*", *Picardie et Champagne-Ardennes, sur le Thème*: "*Recherche Scientifique orientée et transferts de technologie vers les entreprises dans le domaine de la Mécanique*", Compiègne U.T.C., 20 Novembre 1984.

50. Y. Gilibert, *et al., Etude par extensométrie à jauges électriques, par photoélasticimétrie à laser (par transmission), de structures composites collées du type doubles recouvrements symétriques. Comparaison des différents résultats expérimentaux à des calculs analytiques et par éléments finis.* Rapport de Recherche E.N.S.T.A., no. 218, Avril 1987.
51. Y. Gilibert and M. L. L. Klein, "Influence of structure and tensile modulus of adhesive joint, on mechanical strength of metal bonded by various epoxy resins." *Preprints of the First Meeting of the European Polymer Federation,* Lyon, France, September 14–18, 1987.
52. Y. Gilibert and M. L. L. Klein, "Strain gauge and acoustic emission, simultaneous tests of adhesive bonded joints: analysis of mechanical behaviour." Preprints of *"EXPERMAT'87: an International Symposium on Materials with Exceptional Properties"*, Bordeaux, France, November 24–27, 1987, organized by C.E.S.T.A., Paris.